SEARCH FOR MICROFLARING ACTIVITY IN THE MAGNETIC NETWORK

G. CAUZZI[1], A. FALCHI[1] and R. FALCIANI[2]
[1]*Osservatorio Astrofisico di Arcetri, L. Fermi 5, I-50125 Firenze, Italy*
[2]*Dipartimento di Astronomia e Scienza dello Spazio, L. Fermi 5, I-50125 Firenze, Italy*

(Received 30 August 2000; accepted 4 November 2000)

Abstract. We analyze the temporal behavior of network bright points (NBPs) searching for low-atmosphere signatures of flares occurring on the magnetic network. We make use of a set of data acquired during coordinated observations between ground-based observatories (NSO/Sacramento Peak) and the MDI instrument on board SOHO. Light curves in chromospheric spectral lines show only small-amplitude temporal variations, without any sudden intensity enhancement that could suggest the presence of a transient phenomenon such as a (micro)flare. Only one NBP shows spikes of downward velocity, of the order of $2-4$ km s^{-1}, considered as signals of compression associated with a (micro)flare occurrence. For this same NBP, we also find a peculiar relationship between the magnetic and velocity fields fluctuations, as measured by MDI. Only for this point the $B-V$ fluctuations are well correlated, suggesting the presence of magneto-acoustic waves propagating along the magnetic structure. This correlation is lost during the compression episodes and resumes afterward. An A6 GOES soft X-ray burst is temporally associated with the downward velocity episodes, suggesting that this NBP is the footpoint of a flaring loop. This event has a total thermal energy content of about 10^{28} erg, and, hence, belongs to the microflare class.

1. Introduction

High-resolution observations taken by, e.g., *Yohkoh* and SOHO during the solar minimum years have revealed small-scale transient phenomena occurring everywhere on the solar surface. Their presence could have important consequences on the issue of coronal heating: depending on their energy content and distribution, and rate of occurrence, they could provide enough energy to heat the corona (see reviews in Ulmschneider, Rosner, and Priest, 1991). Moreover, if these transient events represent the low energy tail of the broader solar flare family, their study could more easily identify the 'basic' flare mechanisms, not biased by global collective effects as in the case of major solar flares.

Impulsive variations of the emission in the corona or transition region, that could be defined as low-energy flares, have long been observed in both 'quiet-Sun' regions, within magnetic network structures (Golub *et al.*, 1974; Porter *et al.*, 1987), and active regions (Shimizu, 1995). In this paper we will focus on the characteristics of the brightenings associated with the magnetic network.

Krucker *et al.* (1997) observed some small-scale, transient soft X-ray brightening events associated with network magnetic bipoles. These events are spatially and

Solar Physics **199:** 47–60, 2001.

temporally associated with microwave emission, and show several similarities with more energetic flares, such as the same ratio between the total energy emitted in soft X-ray and radio frequencies, etc. However, the total observed radiative losses for these events are more than one order of magnitude smaller than previously reported X-ray events. For these brightenings they introduced the term *soft X-ray network flares*.

Recent SOHO results, based on MDI, EIT, SUMER, and CDS observations, have further demonstrated the highly dynamic nature of the 'quiet magnetic network'. Many observations confirm the existence of EUV brightening events in small-size structures. Harrison (1997) and Harrison *et al.* (1999) observed rapid variations in the emission of transition region lines, associated with junctions of the network magnetic field. The emission characteristics of these brightenings, called blinkers, suggest that they are a class of phenomena distinct from the network flares. Spectrographic observations have shown bursts of highly Doppler-shifted emission, called transition region explosive events (among others, Dere, 1994; Innes *et al.*, 1997; Chae *et al.*, 1998). Chae *et al.* (2000) explored the relationships between blinkers and explosive events. They concluded that although the two phenomena appear different because of the differences in size and duration, they seem to be closely related to each other, for explosive events occur at the edges of blinkers and at the same time. Magnetic reconnection in different magnetic geometries is invoked to explain the observed differences.

Benz and Krucker (1999) and Krucker and Benz (2000) searched for EUV and radio emission variations in non active regions associated with the magnetic network. They observed faint coronal and transition region fluctuations sharing some general properties with more energetic flares (such as the delay between emission originating at different atmospheric layers) and interpreted them as micro- or nano-flares occurring onto the magnetic network.

The investigations mentioned above refer predominantly to coronal and transition region spectral signatures and to photospheric magnetic field measurements. At chromospheric and photospheric levels the bright features associated with the magnetic network do show intensity variations in many spectral signatures (Lites, Rutten, and Kalkofen, 1993; Cauzzi, Falchi, and Falciani, 2000). However, the interpretation for these fluctuations is still an open problem: they might be the result of magneto-acoustic waves which propagate upward along the magnetic lines of force (Hasan and Kalkofen, 1999) or they could represent an instability of the chromosphere itself, as a response to micro or nano-flares processes (Hansteen, 1997). These fluctuations are usually studied in a *statistical* sense and have never been put into direct relation with the network flares identified at higher atmospheric layers.

In this paper we will discuss the search performed at chromospheric and photospheric levels for flares occurring on the magnetic network. Beside the customary analysis of the intensity and velocity variations, we also investigate the changes of the magnetic flux density, and their relation with the fluctuations of the ve-

TABLE I

Summary of the observational set-up. The last column gives the temporal cadence of the corresponding spectral feature.

Instrument	FOV	Spat. resol.	Observing λ (Å)	FWHM (Å)	Δt (s)
UBF	$2' \times 2'$	$0.5'' \times 0.5''$	5889.9 (NaD_2)	0.2	12
			5875.6 (He I D_3)	0.2	
			6562.8 (Hα)	0.25	
			6561.3 (H$\alpha - 1.5$ Å)	0.25	
Zeiss	$2' \times 2'$	$0.5'' \times 0.5''$	6564.3 (H$\alpha + 1.5$ Å)	0.25	3
White light	$2' \times 2'$	$0.5'' \times 0.5''$	5500	100	3
HSG	$0.75'' \times 2'$	$0.75'' \times 0.36''$	3904–3941 (Ca II K)	0.035	–
		$0.75'' \times 0.13''$	4094–4108 (Hδ)	0.011	–
MDI	$10' \times 6'$	$0.6'' \times 0.6''$	6768 Ni I	0.1	60

locity field. We use a subset of the high spatial resolution observations obtained in August 1996 during a coordinated observing program between ground based observatory ('R. B. Dunn' Solar Telescope at NSO/Sacramento Peak) and the Solar and Heliospheric Observatory (SOHO).

2. Observations and Data Reduction

Table I reports a summary of the observing setup, more accurately described in Cauzzi *et al.* (1997, 1999). We give here only some short information for the data used in this paper. Monochromatic intensity images were obtained with the tunable universal birefringent filter (UBF) and the Zeiss filter, at high spatial and temporal resolution. Spectra have been acquired with the horizontal spectrograph (HSG) around the Ca II K and Hδ lines, setting the slit in different positions within the field of view (FOV). On board SOHO, the Michelson Doppler Imager (MDI, Scherrer *et al.*, 1995) acquired data with an image scale of $0.605''$ pixel^{-1}. Maps of continuum intensity, line-of-sight velocity and longitudinal magnetic flux were obtained in the Ni I 6768 Å line at a rate of one per minute for several hours. The velocity images were available with a binned 2×2 format. The different spectral signatures allow a good coverage of the whole photospheric-chromospheric region.

The data analyzed in the present paper were obtained on 15 August 1996, when we had a period of constant good seeing conditions (better than $1''$) during one hour (15:15–16:05 UT). The MDI data were considered for a longer interval, 14–17 UT. A small active region (AR NOAA 7984), with a very low activity level, was present in the field of view. Some pores and a small spot were the prominent structures in the white light and continuum images, and have been used for co-alignment of the whole dataset. At each given time the alignment among the images acquired

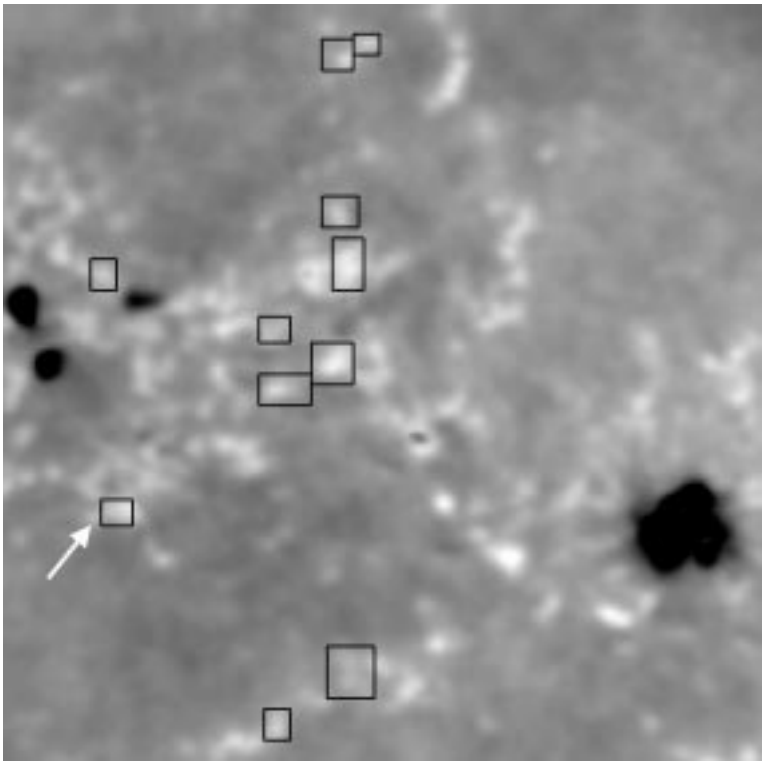

Figure 1. NaD_2 image of the FOV, averaged over the period 15:15–16:05 UT, 15 August 1996. The bright pattern closely overlays the network magnetic structure (Cauzzi, Falchi, and Falciani, 2000). The black squares indicate the 11 NBPs analyzed. The arrow indicates the peculiar NBP considered in the following.

with different instruments was better than about $1''$. We refer to Cauzzi, Falchi, and Falciani (2000) for details on FOV overlay and data reduction procedures.

The magnetic network structure was clearly visible within the FOV in several sets of images (MDI magnetic maps; NaD_2 intensity; Hα wings). We searched for activity manifestations on several network bright points (NBPs), sharing the following properties: bright in the Ca II wings and in the Ca II K_2 peaks; visible in the NaD_2 images for about 1 hr; spatially coincident with magnetic structures. We identified a total of 11 NBPs with the required characteristics, displayed in Figure 1. We did not consider other bright points visible in the FOV, since no corresponding Ca II K spectra were available.

3. Flaring Activity on the Magnetic Network

3.1. Intensity and velocity analysis

As a first step, we searched for the presence of flaring episodes within the network by analyzing the intensity light curves, obtained separately for each NBPs and each spectral signature. Light curves were obtained setting an intensity threshold for each signature, and averaging over the spatial pixels that exceeded this threshold (more details can be found in Cauzzi, Falchi, and Falciani, 2000). For the white light, Ni I continuum, and He I-D_3 images no intensity threshold could clearly discriminate between NBPs and surrounding areas, within the limits of our statistical photometric precision ($\approx 0.5\%$).

In Figure 2, as an example, we show light curves of different signatures for two network bright points. The variations of the emission are small in amplitude and semi-regular in their temporal distribution. None of the analyzed NBPs displays any sudden intensity enhancement that could suggest the presence of a transient phenomenon such as a microflare. A search for the presence of regular fluctuations has been performed in Cauzzi, and Falchi, and Falciani (2000) and reveals different temporal frequencies for different spectral signatures.

The fluctuations in different spectral signatures are not clearly in phase with each other (see Figure 2). An exception is represented by the H$\alpha \pm 1.5$ Å wings light curves (Figure 2, left). The evolution of most NBPs in the red and blue wings of Hα is very similar, with simultaneous intensity variations of the same amplitude, between 0.5 and 1.5% of their average values. This similarity indicates that velocity fluctuations do not play a role in the observed intensity variations, and that these are most likely related to temperature or density fluctuations.

However, one of the analyzed NBPs displays out-of-phase intensity variations in the wings of Hα, that could be explained by an asymmetric absorption profile (see Figure 2, right). The hypothesis of an Hα absorption profile seems reasonable, since the light curves obtained in the Hα center do not show any particular enhancement at any time and the Hδ spectra acquired on several NBPs at different times always show an absorption profile.

Interpreting the difference in intensity as due to a velocity field (as commonly done in Dopplergrams), we derived the line-of-sight velocity corresponding to the layers that contribute to the Hα wings.

In Figure 3 we show this velocity as a function of time for this particular NBP (top panel) and for one 'typical' NBP (bottom panel). The peculiar NBP displays three spikes of downward velocity within the interval 15:25–15:45 UT, with a typical lifetime of about 1.5 min. The amplitude of these spikes is well above the error estimated at about 1 km s^{-1}.

A downward motion measured in Hα or other chromospheric lines represents a typical signature during the impulsive phase of a flare (Ichimoto and Kurokawa, 1984). This motion is due to the sudden compression of the lower atmosphere

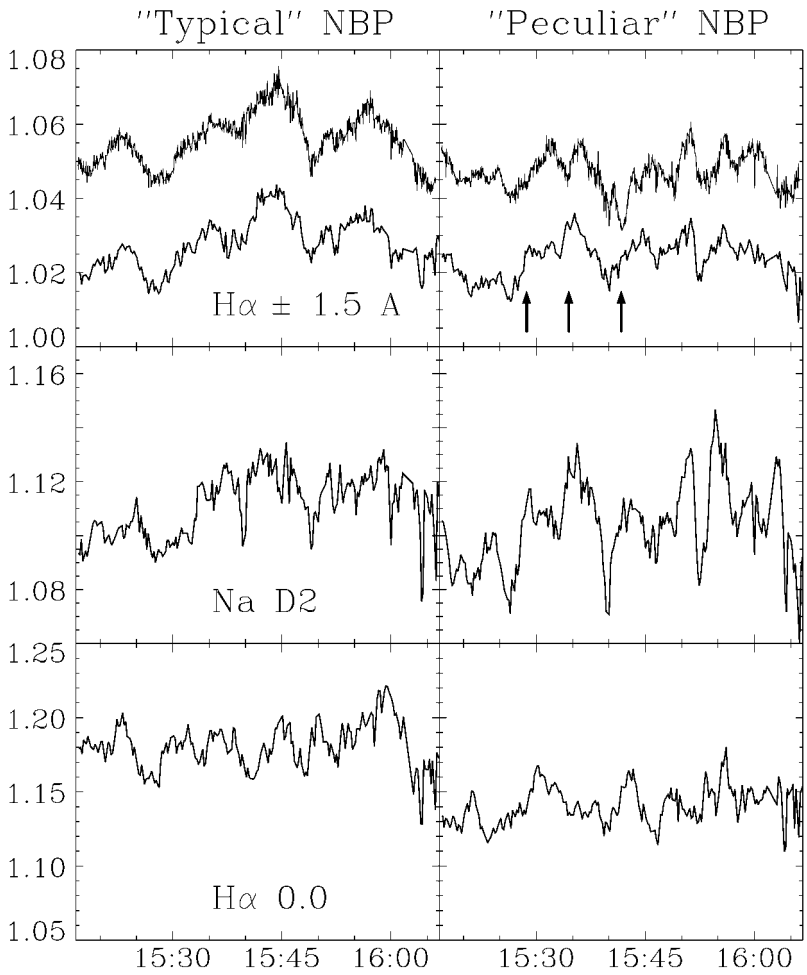

Figure 2. Intensity light curves, obtained in several spectral signatures, for two NBPs. The curves are normalized to the quiet average value and long-period trends have been subtracted. In the first row the higher curve (shifted upward by 0.03 for clarity) represents the Hα + 1.5 Å emission. *Left column*: 'typical' NBP with simultaneous intensity variations in the Hα wings. *Right column*: the only NBP showing non-correlated variations in the Hα wings (indicated by arrows).

caused by either a particle beam or a conduction front. This has been proved also for small-size events, such as the microflares described by Canfield and Metcalf (1987) as the Hα counterparts of hard X-rays burst. Hence, we can suppose that these downward velocity episodes represent the signature of the occurrence of flare processes within this peculiar NBP.

The MDI velocity fluctuations measured in this area (Figure 3, thicker line) are comparable with those registered in any other NBP and, in particular, do not show any peak in correspondence with the downward motions registered in the Hα wings. Probably, within the flare-driven chromospheric condensation, the Hα

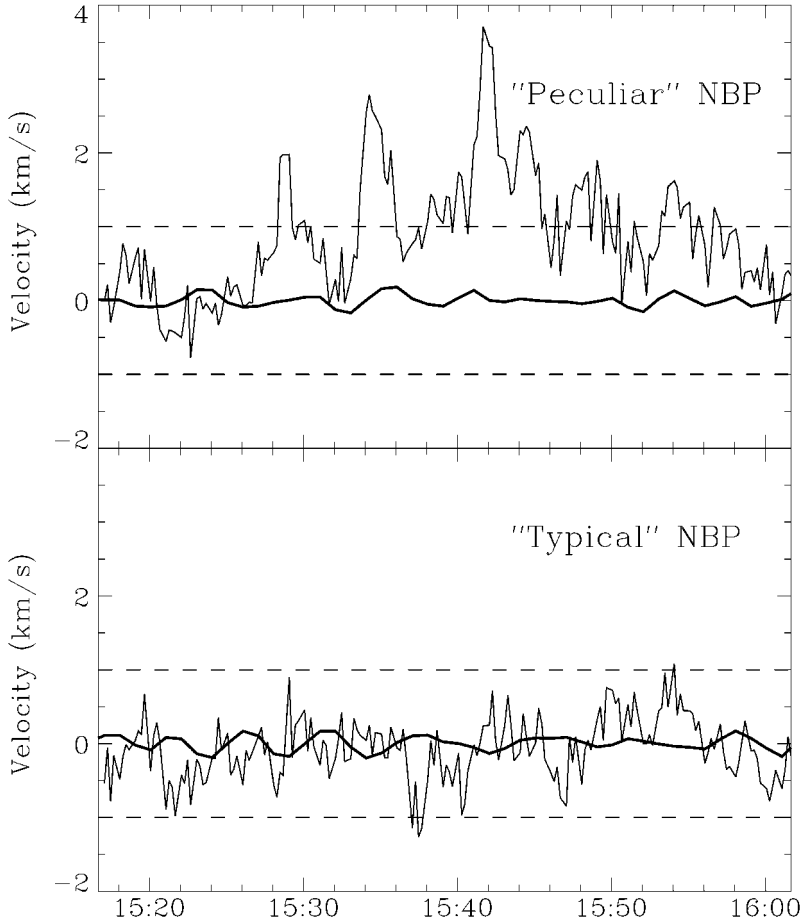

Figure 3. Top: line-of-sight velocity distribution (positive values indicate downward motions) for the particular NBP described in text. *Bottom*: line-of-sight velocity distribution for one typical NBP. *Thin line*: Hα wings velocity, with the error bar indicated by the *dashed lines*. *Thick line*: MDI-Ni I velocity, $\pm$ 0.2 km s^{-1}.

wings originate from higher atmospheric levels than the Ni I line used by MDI, and are more sensitive to the disturbances introduced by a flare.

3.2. VELOCITY AND MAGNETIC FIELD CORRELATION

This NBP coincides on the MDI maps with a magnetic structure of negative polarity with a flux density smoothly increasing in time from 150 to 250 G. Some very weak structures of opposite polarity, barely above the noise (15 G), are present in the surroundings.

In general, within the NBP areas both the magnetic flux density (B) and the line of sight velocity (V) fluctuate with a rough periodicity of 5 min, but these fluctuations do not appear to be related to each other (see Cauzzi, Falchi, and

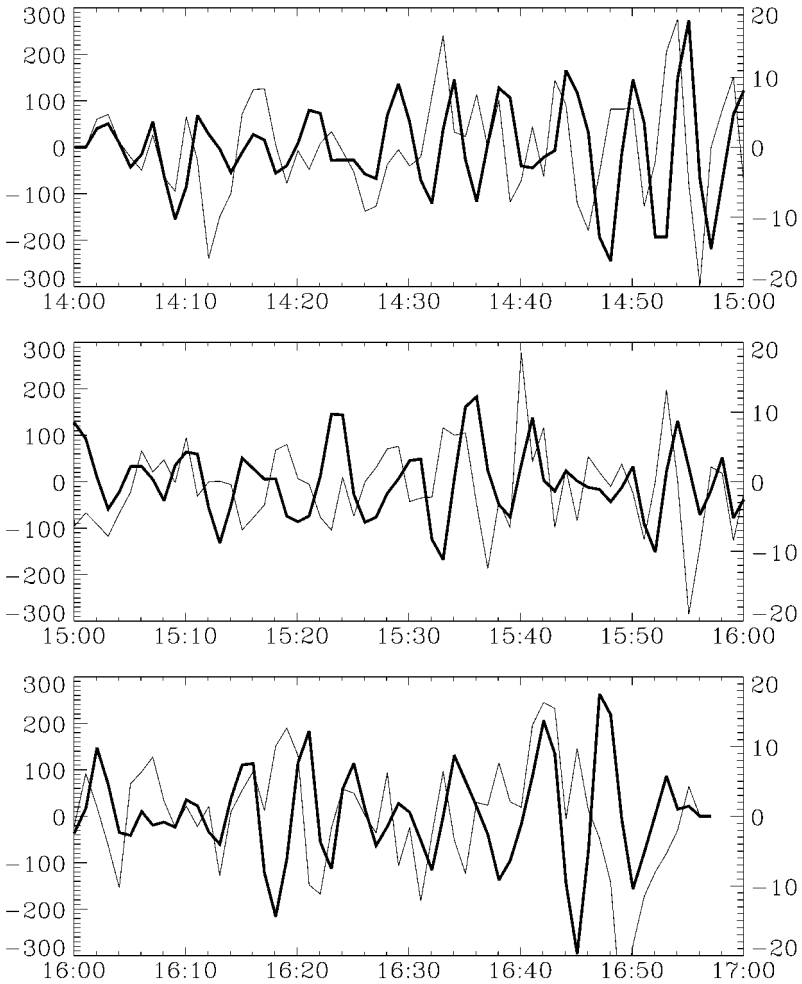

Figure 4. Comparison between the fluctuations of the MDI line-of-sight velocity (*thick line*, scale on the left in m s^{-1}) and of the longitudinal magnetic flux density (*thin line*, scale on the right in G). For both quantities the average value and the long period trends have been subtracted.

Falciani, 2000, for further details). For this particular NBP, the B and V fluctuations are instead well correlated for long periods of time, 14:00–15:10 UT and 15:40–17:00 UT (see Figure 4). However, during the interval 15:10–15:40, when also the Hα downward motions are measured (see Figure 4), their correlation gets smaller.

These characteristics are confirmed by a more accurate analysis, that makes use of the phase difference (Φ) and the coherence (C) spectra in the Fourier domain for the pair $B - V$ (see Edmonds and Webb, 1972 for definition of Φ and C). Basically, the phase difference provides a measure of the delays between periodic signals, while the coherence gives the persistence of this phase difference. Reliable values of phase difference can be given only if C has values higher than about 0.9.

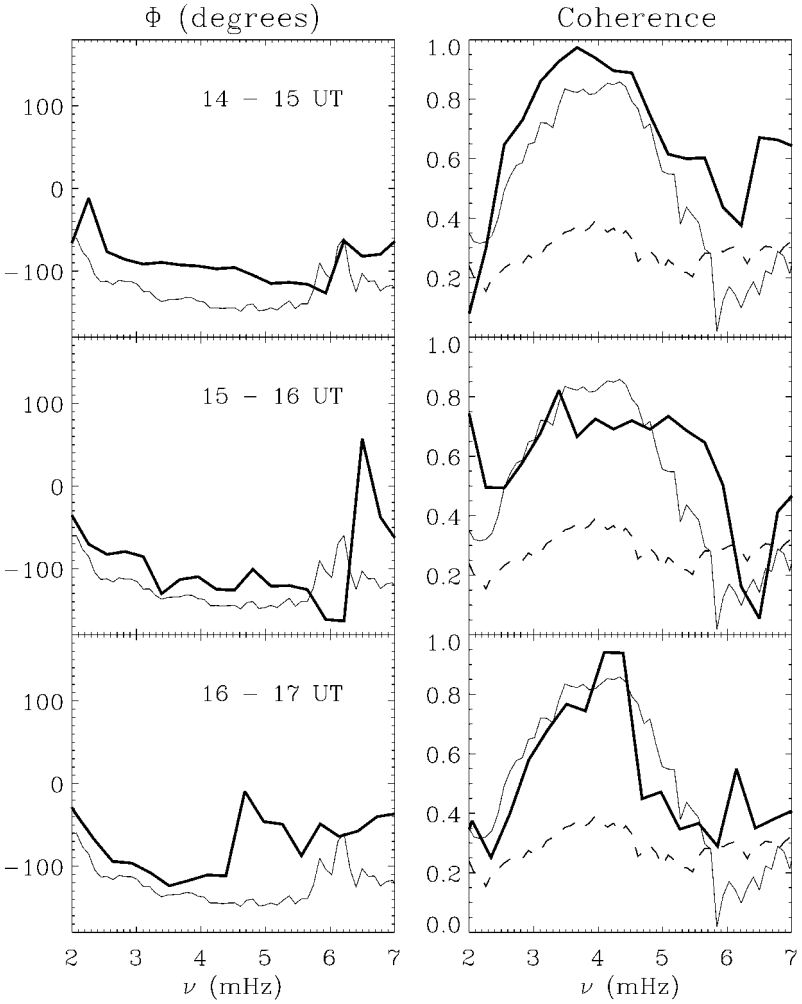

Figure 5. $B - V$ phase difference (*left*) and coherence (*right*) spectra. *From top to bottom*: the spectra (*thick line*) are shown for three consecutive time windows: 14–15, 15–16, and 16–17 UT. The *thin line* represents the average over the whole 3-hr period for the flaring NBP, while the *dashed line* is an average for the remaining 10 NBPs.

In Figure 5 (left) we show the phase difference $B - V$ for the peculiar NBP, as a function of the temporal frequency, computed for the whole observing period and for three separated periods of one hour each. For this calculation we considered positive the upward velocity, as it is customary. The corresponding coherence spectra are shown in Figure 5 (right). The coherence spectrum shows a peak of about 0.95 at the frequency corresponding to 5-min oscillations in the time intervals 14 –15 UT and 16–17 UT. This maximum is lowered to about 0.7–0.8 during the period 15–16 UT, when B and V lose their correlation (Figure 4). At the frequency of the maximum coherence the phase difference is of about $-90°$, with the

upward velocity V leading B. This is consistent with the presence of propagating magneto-acoustic waves within this magnetic area (Ulrich, 1996), possibly excited by granular buffeting of the magnetic elements (Hassan and Kalkofen, 1999). For all the other NBPs the $B - V$ coherence spectra assume very low values (Figure 5, dashed), and hence no phase difference analysis can be performed.

The lack of coherence between B and V fluctuations in the majority of NBPs could be explained by the magnetic field configuration in the network. As shown for example by Schrijver *et al.* (1997), the network magnetic cells consist of a large number of very small concentrations of mixed polarities, connected mostly via short loops. In such small structures, wave reflections or distortion can destroy the coherence between B and V fluctuations, not allowing the persistence of any phase difference. The particular NBP where we observe a definite phase difference, might instead be connected to the opposite polarity via a longer loop that hence allows wave propagation.

As said above, in this NBP the coherence between B and V is reduced during the interval 15:10–15:40 UT (Figure 4). The temporal coincidence with the Hα downward motions suggests that the same phenomenon can be responsible also for this disturbance. If the downward motions measured in Hα are a signature of a flare, one can suppose the occurrence of magnetic reconnection processes involving this longer loop and having strong effects on the footpoint(s). During a reconnection process, the magnetic topology changes abruptly and any oscillations regime of B would be strongly perturbed. As a result, the wave propagation will be disrupted and the $B - V$ coherence reduced. The phase difference between the fluctuations could then be re-established once the perturbation is over. The MDI maps show some weak magnetic structures of opposite polarity in the vicinity of this NBP within the considered temporal interval. Any of these structures could be involved in the reconnection process, but the complexity of the 'salt and pepper' magnetic pattern makes it impossible to identify the particular feature involved.

3.3. SOFT X-RAY BURST

The scenario outlined in the previous sections of a magnetic reconnection and a sudden compression at low atmospheric layers suggests the possibility of associated emission coming from higher atmospheric layers. Hence, we searched for coronal signatures temporally and/or spatially associated with these signals from the lower atmosphere. Unfortunately, during the considered time lag *Yohkoh* was in its night-time and only SXT full-disk frames were available before and after this interval. Two active regions were present on the disk: NOAA 7982 at the west limb and NOAA 7984, visible in our FOV. An accurate analysis of the images available for both regions, for two hours before and one hour after, reveals that the SXR emission of NOAA 7982 was decreasing very slowly during the whole period, while NOAA 7984 showed global intensity fluctuations of about $\pm$ 2% hr^{-1}.

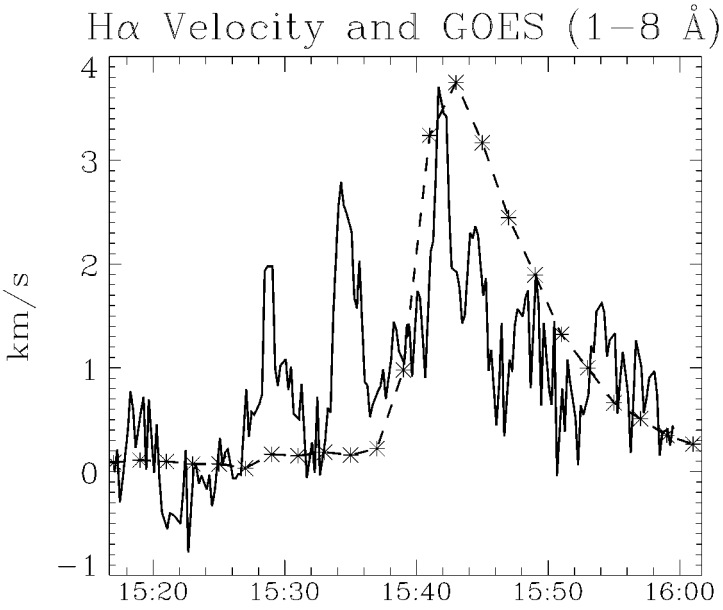

Figure 6. SXR emission from GOES 1−8 Å band (*dashed line*, relative units), superimposed with Hα line-of-sight velocity.

This suggests that only the region present in our FOV can show some episodes of activity.

GOES recorded an A6 burst in both channels (0.5−4 and 1−8 Å), with maximum peak at 15:43 UT. The temporal evolution of the SXR emission in the 1−8 Å band is shown in Figure 6, superimposed with the line-of-sight velocity outbursts deduced from the Hα wings. The temporal coincidence between the two curves is good. The first two velocity spikes, of small amplitude, correspond to a modest increase of the SXR emission (build-up phase), while the third, larger one, corresponds to the peak of the GOES curve. If we accept the suggestion that only the AR present in our FOV can display activity, this particular NBP most probably is the footpoint of a flaring loop.

Following Thomas, Starr, and Crannell (1985), from the ratio of the GOES channels power fluxes (0.5−4 Å/1−8 Å), we can estimate an electron temperature T_e of about 4.5 MK and an emission measure EM of about 10^{47} cm^{-3}. Assuming a mean electron density of 10^{10} cm^{-3}, (typical of dense coronal loops) we can estimate a mean volume of 10^{27} cm^3 for the plasma emitting the measured SXR burst. A cylindrical coronal loop, with a constant diameter of 5″ (somewhat larger than this NBP to take into account the possible size increase of magnetic structures at coronal levels), would have a total length of 8×10^4 km, with a total thermal energy content of about 10^{28} erg. Hence, in a completely independent way, we again suggest the presence of a long magnetic loop with a footpoint in a network bright area. The values found for T_e, for the EM, and for the associated thermal

energy for this SXR event are consistent with those quoted by Feldman, Doschek, and Behring (1996) for microflares of A6 GOES type. We can then conclude that this event can be considered as a real *network microflare*.

4. Conclusions

We searched for the presence of chromospheric and photospheric signatures of low-energy flares occurring on the magnetic network. Eleven NBPs, each one corresponding to a patch of definite polarity, were selected in a $2' \times 2'$ field of view, where also a small and low-activity region was present. The intensity fluctuations of several spectral signatures observed for the NBPs do not show any impulsive episodes typical of the flare occurrence. The general characteristics found for these NBPs do not differ from the ones derived in quiet regions (Cauzzi, Falchi, and Falciani, 2000). Only for one NBP we found two peculiar characteristics:

–The intensity fluctuations in the Hα wings ($\pm$ 1.5 Å) are not in phase for about 20 min. From the difference of the intensity of the Hα wings we derived the corresponding velocity and found that three spikes of downward motions (respectively of 2.0, 2.7, and 3.7 $\pm$ 1.0 km s^{-1}) occurred within this interval. Plasma motions of this kind are generally considered as a signature of sudden compression of the lower atmosphere, typical of flares.

–In the Fourier domain, at the frequency corresponding to 5-min oscillations, the MDI magnetic and velocity fluctuations in this NBP show a coherence spectrum with a high value ($\approx$ 0.8, see Figure 5) when compared to the average for all the other NBPs ($\approx$ 0.4). Analyzing the coherence spectrum for 3 separate periods, we found that before and after the downward velocity episodes, the coherence has an even higher value of about 0.95, while just during the sudden compression episodes, the coherence is lowered to 0.7. We suggest that a reconnection process, that might be responsible for the sudden compression indicated by the three spikes of downward velocity, might also destroy the coherence of magneto-acoustic waves propagating along the magnetic field lines of a long loop connecting this NBP with a distant opposite polarity.

GOES recorded an A6 burst in both channels, that temporally coincides with the stronger downward velocity spike. We derived $T_e = 4.5$ MK and $EM \approx 10^{47}$ cm^{-3} for a coronal loop with a constant diameter of $5''$ and a total length of about 8×10^4 km.

The general picture emerging from the data is hence the following: the particular network bright point examined is connected via a long magnetic loop to a distant opposite polarity structure. In ‘quiet’ conditions, magneto-acoustic waves can propagate along this loop as derived from the $-90°$ phase difference measured between B and V fluctuations. Magnetic reconnection involving this loop disrupts the coherence between these fluctuations, and produces the compression episodes observed in the lower atmosphere. At coronal levels the simultaneous increase in

SXR emission might identify the corresponding chromospheric evaporation. All this evidence points toward the occurrence of a real 'network flare'. Contrary to more energetic flares, for such an event a sudden intensity increase does not represent a characteristic signature in the low atmosphere. Instead, downward motions seem to be a common property for both larger and smaller flares. An intriguing characteristic of this particular flare is given by the disruption of the coherence between the B and V fluctuations. This is the first time that such a property is observed, so it would be premature to comment on its relevance as a flare signature. Further investigation on the subject is desirable.

Acknowledgements

The authors express their warmest thanks to the MDI team (P.I., P. H. Scherrer) for the efficient support during the observing run. The support of the NSO/Sacramento Peak 'R.B. Dunn' Tower staff was essential for getting good data. The authors would like to thank Drs E. Landi and M. Velli for helpful collaboration and stimulating discussions.

References

Benz, A. O. and Krucker, A.: 1999, *Astron. Astrophys.* **341**, 286
Canfield, R. C. and Metcalf, T. R.: 1987, *Astrophys. J.* **321**, 586.
Cauzzi, G., Falchi, A., and Falciani, R.: 2000, *Astron. Astrophys.* **357**, 1093.
Cauzzi, G., Vial, J. C., Falciani, R., and Falchi, A.: 1997, in B. Schmieder, J. C. del Toro Iniesta, M. Vázquez (eds.), *ASP Conf. Ser.* **118**, p. 309.
Cauzzi, G., Falchi, A., Falciani, R., and Vial, J. C.: 1999, in A. Wilson (ed.), *Magnetic Fields and Solar Processes, 9th EPS Solar Meeting*, Florence, ESA SP-448, p. 685.
Chae, J., Lee, C.-Y., Wang, H., Goode, P. R., and Schühle, U.: 1998, *Astrophys. J.* **497**, L109.
Chae, J., Wang, H., Goode, P. R., Fludra, A., and Schühle, U.: 2000, *Astrophys. J.* **528**, L119.
Dere, K. P.: 1994, *Adv. Space Res.* **14**, 13.
Edmonds, F. N., Jr. and Webb, C. J.: 1972, *Solar Phys.* **22**, 276.
Feldman, U., Doschek, G. A., and Behring, W. E.: 1996, *Astrophys. J.* **461**, 465.
Golub, L., Krieger, A. S., Silk, J. K., Timothy, A. F., and Vaiana, G. S.: 1974, *Astrophys. J.* **189**, L93.
Hansteen, V.: 1997, in A. Wilson (ed.), *The Corona and Solar Wind Near Minimum Activity*, Fifth SOHO Workshop, Oslo, 17–20 June 1997, ESA SP-404, p. 45.
Harrison, R. A.: 1997, *Solar Phys.* **175**, 457.
Harrison, R. A., Lang, J., Brooks, D. H., and Innes, D. E: 1999, *Astron. Astrophys.* **351**, 1115.
Hasan, S. S. and Kalkofen, W.: 1999, *Astrophys. J.* **519**, 899.
Ichimoto, K. and Kurokawa, K.: 1984, *Solar Phys.* **93**, 105.
Innes, D. E., Brekke, P., Germerott, D., and Wilhelm, K.: 1997, *Solar Phys.* **175**, 341.
Krucker, S. and Benz, A. O.: 2000, *Solar Phys.* **191**, 341.
Krucker, S., Benz, A. O., Bastian, T. S., and Acton, L. W.: 1997, *Astrophys. J.* **488**, 499.
Lites, B. W., Rutten, R. J., and Kalkofen, W.: 1993, *Astrophys. J.* **414**, 345.
Porter, J. G., Moore, R. L., Reichmann, E. J., Engvold, O., and Harvey, K. L.: 1987, *Astrophys. J.* **323**, 380.

Scherrer, P. H. *et al.*: 1995, *Solar Phys.* **162**, 129.
Schrijver, C. J., Title, A. M., van Ballegooijen, A. A., Hagenaar, H. J., and Shine, R. A.: 1997, *Astrophys. J.* **487**, 424.
Shimizu, T.: 1995, *Publ. Astron. Soc. Japan* **47**, 251.
Thomas, R. J., Starr, R., and Crannell, C. J.: 1985, *Solar Phys.* **95**, 323.
Ulmschneider, P., Rosner, R., Priest, E. R. (eds.): 1991, *Mechanisms of Chromospheric and Coronal Heating*, Springer-Velag, Berlin.
Ulrich, R. K.: 1996, *Astrophys. J.* **465**, 436.